LIQUID CRYSTALS, 1993, VOL. 14, NO. 2, 389–404

Computer simulation of the electro-optical switching process in ferroelectric liquid crystal cells with bookshelf geometry

by F. GIEßELMANN and P. ZUGENMAIER*
Institut für Physikalische Chemie der TU Clausthal, Arnold-Sommerfeld-Straße 4, D-3392 Clausthal-Zellerfeld, Germany

The electro-optical properties of a ferroelectric liquid crystal in thin surface stabilized cells with bookshelf geometry were studied with respect to the temperature and to the frequency with alternating amplitude and waveform of the electric field applied. Using a previously proposed model of director reorientation, the measurements were simulated, and a consistent description of the electro-optical behaviour of the system achieved. The fit of the simulations to the measurements provided material constants for the compound investigated and these are discussed.

1. Introduction

In thin cells, the chiral smectic C phase (S_C^*) exhibits ferroelectric properties [1, 2]. The direction of the spontaneous polarization depends on the position of the director relative to the layer normal. Therefore, an alternating electric field with sufficient amplitude induces a director reorientation through coupling with the spontaneous polarization and leads to interesting electro-optical properties of the S_C^* phase [3].

Electro-optical measurements allow the experimental determination of the trajectory described by the director during the reorientation [4, 5] in copolar coordinates ϑ_s (off-plane angle), φ_s (in-plane angle) relative to the substrate plane of the cell in a laboratory coordinate system (see figure 1), if the switching process can be described as optically uniform. The laboratory coordinate system is related to the S_C^* coordinate system by the smectic layer tilt angle δ [6, 7].

The trajectories are theoretically available by an integration of the equations of motion of a proposed model. A fit to the experimental data allows then a simultaneous determination of several material and cell constants [7, 8]. The knowledge of these data leads to the theoretical transmission curve of the electro-optical measurement which can be compared with that determined experimentally.

2. Model of director reorientation

A dynamical model for director reorientations in surface stabilized ferroelectric liquid crystal cells, which in addition includes a reorientation of the smectic layers has been proposed in a previous paper [7] and was successfully applied. A brief summary of the model will be given in order to outline the basic ideas leading to the simulation procedure.

The proposed dynamical model uses a simplified description of the director distribution across the cell thickness which is schematically drawn in figure 2. The cell of thickness d is divided into several layers, and boundary conditions related by C_2 symmetry (parallel rubbed glass plates) are introduced. The top boundary layer (tb), the

* Author for correspondence.

0267–8292/93 $10·00

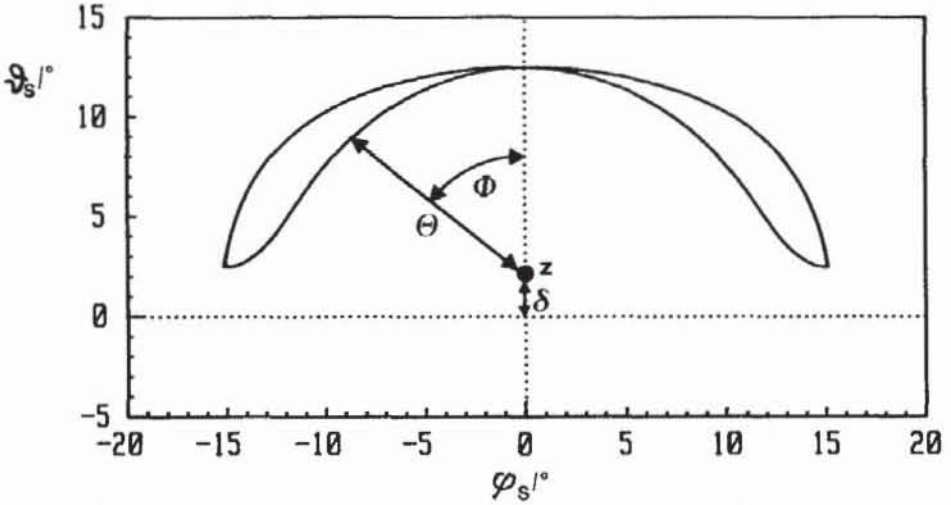

Figure 1. Description of director reorientations by trajectories in a laboratory coordinate system. The different director orientations which are passed through during the reorientation are described by an in-plane angle φ_s and an off-plane angle ϑ_s, which are related to the substrate plane along $\vartheta_s = 0°$. The relation to the S_C^* coordinate system is given by the smectic layer normal **z** at $\varphi_s = 0°$, which exhibits a layer tilt angle δ with the substrate plane. The angular distance between **z** and a certain point of the trajectory represents the corresponding director tilt angle Θ. The tilt direction is given by the azimuthal angle Φ.

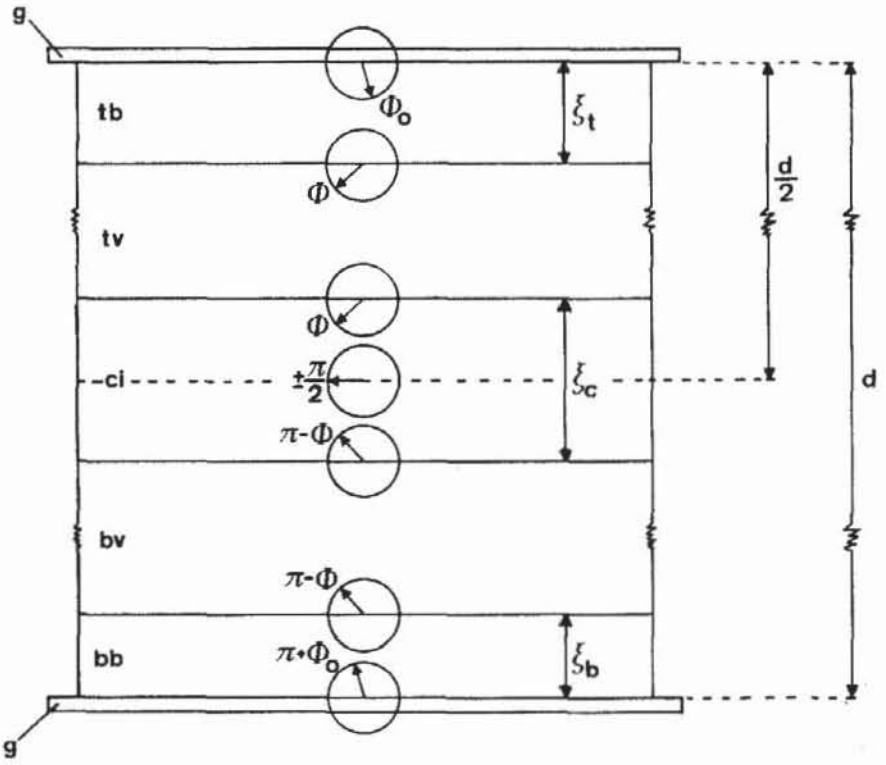

Figure 2. Proposed model for a description of the director configuration of a ferroelectric liquid crystal cell under an applied electric field. Explanations are in the text.

bottom boundary layer (bb) and the chevron interface (ci) with thicknesses ξ_t, ξ_b, and ξ_c, respectively, are assumed to be sections with a non-uniform, linearly varying director distribution. The top and the bottom volume layer (tv and bv in figure 2) are considered as sections exhibiting a uniform director configuration. The elastic energy of the cell is located within the non-uniform sections tb, bb and ci, whereas the energy resulting from the **P**, **E** interaction is predominantly located in the uniform layers tv and bv. By competition between elastic and electric forces during the director reorientation, the borderlines between the several layers are allowed to travel back and forth throughout the cell. This propagation of the splay deformation is dampened by a viscous constant γ_{splay}.

If the director is anchored at the upper boundary at an azimuthal angle Φ_0, the azimuthal angle at the lower boundary is $\pi+\Phi_0$ (see figure 2) and the total splay distortion across the cell amounts to π. Due to polar interactions between the ferroelectric liquid crystal and the substrates, ferroelectric liquid crystal cells exhibit complex non-uniform director configurations [9]. Under the conditions of a sufficiently strong electric field, these non-uniform configurations transform into director configurations which appear optically uniform.

If no or only a small electric field is applied, the uniform sections tv and bv vanish and the cell exhibits an overall non-uniform director distribution ($\xi_t+\xi_b+\xi_c=d$). On the other hand, the total thickness of the non-uniform layers may become very small compared to the cell thickness ($\xi_t+\xi_b+\xi_c \ll d$) under electric field conditions. Therefore, the cell appears uniform and its electro-optical behaviour is described by the electro-optical behaviour of the uniform sections tv and bv to a good approximation.

This model leads to the following Gibbs free energy expansion [7] with ferroelectric, elastic, and collective dielectric interactions as a function of the internal coordinates Θ (director tilt angle), Φ (azimuthal angle), δ (layer tilt angle), the thicknesses ξ_t, ξ_b, and ξ_c, and the applied electric field E considered

$$\begin{aligned} g-g_0 = {} & \tfrac{1}{2}a\Theta^2+\tfrac{1}{4}b\Theta^4+\tfrac{1}{6}c\Theta^6 \\ & +\frac{K_{\text{splay}}\Theta^2\cos^2\delta}{2d}\left[\frac{(\Phi_0-\Phi)^2}{\xi_t}+\frac{(\pi-2|\Phi|)^2}{\xi_c}+\frac{(\Phi_0+\Phi)^2}{\xi_b}\right] \\ & -\left(1-\frac{\xi_t+\xi_c+\xi_b)}{d}\right)\Bigg[P_0E\sin\Theta\cos\delta\sin\Phi \\ & +\frac{\epsilon_0E^2}{2}(\Delta\epsilon_G\cos^2\Phi+\Delta\epsilon_S\sin^2\Phi)\cos^2\delta\Bigg], \end{aligned} \tag{1}$$

where a, b, c are coefficients of the Landau expansion, K_{splay} is a splay elastic constant, P_0 is a coupling constant of the spontaneous polarization, $\Delta\epsilon_G$ is the relative dielectric strength of the Goldstone mode, and $\Delta\epsilon_S$ is the relative dielectric strength of the soft mode. Introduction of dissipation terms leads to the equations of motion:

$$\gamma_\Theta\frac{d\Theta}{dt}=-\left(\frac{\partial g}{\partial\Theta}\right), \tag{2a}$$

$$\gamma_\Phi\sin^2\Theta\frac{d\Phi}{dt}=-\left(\frac{\partial g}{\partial\Phi}\right), \tag{2b}$$

$$\gamma_\delta \frac{d\delta}{dt} = -\left(\frac{\partial g}{\partial \delta}\right), \tag{2c}$$

$$\gamma_{\text{splay}} \frac{d\xi_t}{dt} = -\left(\frac{\partial g}{\partial \xi_t}\right), \tag{2d}$$

$$\gamma_{\text{splay}} \frac{d\xi_c}{dt} = -\left(\frac{\partial g}{\partial \xi_c}\right), \tag{2e}$$

$$\gamma_{\text{splay}} \frac{d\xi_b}{dt} = -\left(\frac{\partial g}{\partial \xi_b}\right), \tag{2f}$$

where γ_Θ, γ_Φ, γ_δ and γ_{splay} are viscous damping constants related to the motion of the director in Θ, Φ, the smectic layers in δ and the propagation of the splay deformation in ξ_t, ξ_b, ξ_c. respectively.

The set of differential equations (2 *a–f*) may be solved numerically by a 4th order Runge-Kutta algorithm, and the solutions transformed into the laboratory coordinate system (cf. figure 1) and converted into the corresponding transmission curves. The calculated trajectories and transmission curves are compared with experimental results, and variation of the several constants leads to a best fit towards the experimental data. The experiments considered in this investigation have been carried out with surface stabilized ferroelectric liquid crystal cells which were irreversibly reoriented from a chevron into a bookshelf structure ($\delta \approx 0°$) by high electric field treatment [6, 7, 10–12]. In bookshelf cells, which are obtained from electrically reoriented chevron cells, the chevron interface remains as a local mirror plane [13] and the described model, which originally referred to chevron cells, can be applied with $\delta \approx 0$. The layer orientation is fixed after completing the high field treatment [6, 7], and consequently, equation (2 *c*), describing a layer reorientation, is not considered for the simulations presented in this paper.

3. Experimental

Electro-optical experiments were carried out on a commercially available 4 μm cell (E.H.C. Co. Ltd., Tokyo) with polyimide coating and filled with *S*−(+)−4−[2-chloro-3-methylbutyryloxy]phenyl-4-decycloxybenzoate [14] (phase sequence: C S_C^* 44–45°C) S_A^* 64°C I). The refractive indices, necessary for an evaluation of the optical data, were supplied by Dr G. Pelzl (Martin-Luther-Universität, Halle-Wittenberg). The exact thickness of the cell was determined as 3·85 μm by the interference spectrum of the empty cell with application of the corrections given by Yang [15], with consideration of the optical influence of the polyimide and ITO layers. After slowly cooling from the isotropic phase, a well oriented S_C^* phase was obtained, and the cell exhibited a chevron layered structure. The initial chevron structure was irreversibly transformed into a bookshelf structure by application of a strong electric square field with an amplitude of 15 MV m^{-1} and a frequency of 200 Hz [6, 7]. The experimental set-up used for the measurements is described elsewhere [4, 5]. Simulations were carried out using a Hewlett–Packard 9000/382 workstation. The calculation of a trajectory and the corresponding transmission curve required about 30 s, if 2000 data points were considered. Typically 20 runs were necessary to obtain a stationary solution.

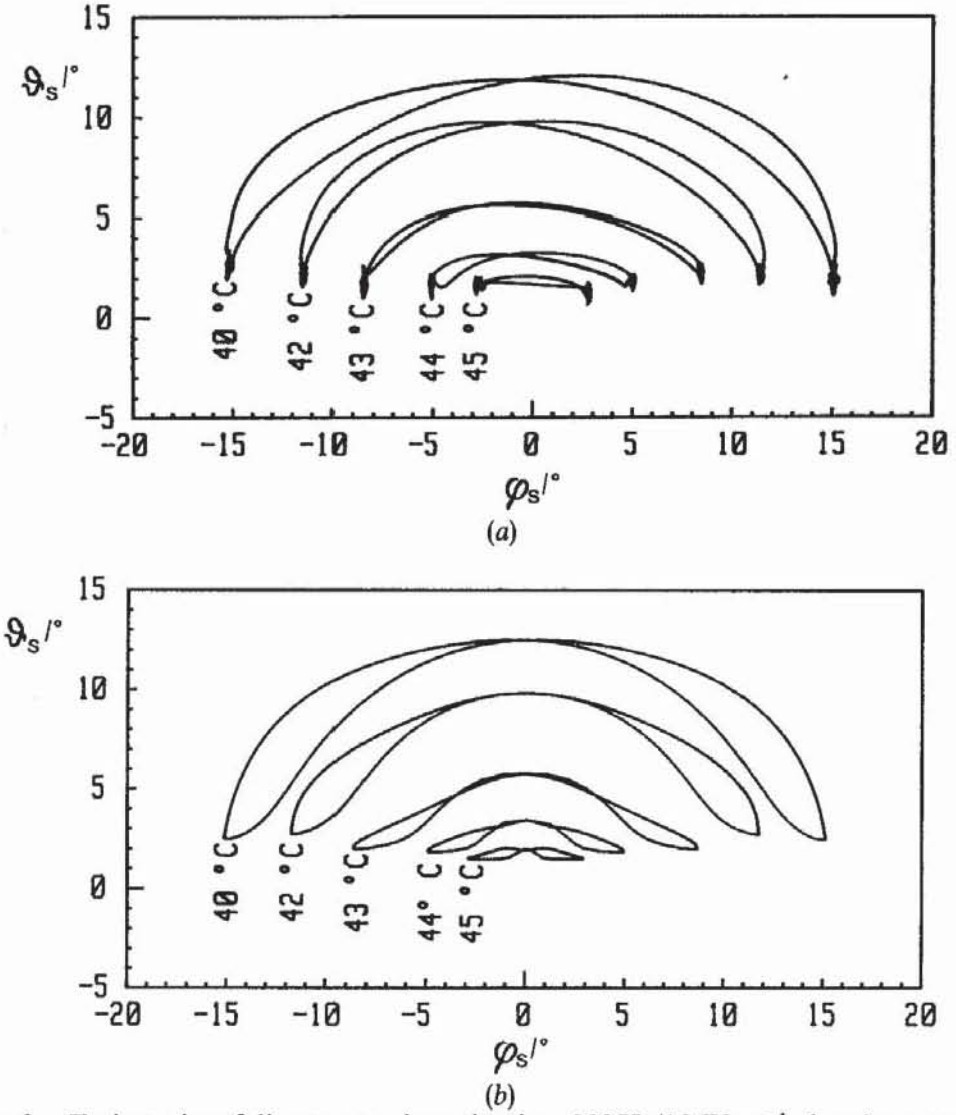

Figure 3. Trajectories of director reorientation in a 200 Hz/1 MV m^{-1} electric square field at various temperatures. (*a*) Trajectories determined experimentally by electro-optical measurements. (*b*) Trajectories simulated theoretically by the proposed model.

4. Results and discussion

The influence of the applied electric field (shape, amplitude and frequency) and of the temperature on the electro-optical behaviour were studied and the measurements compared with simulations based on the proposed model. Some representative results will be discussed. Preceding investigations on the influence of the cell treatment with respect to the formation of a bookshelf geometry in high electric fields are reported in [7].

4.1. *Temperature dependence*

Figure 3 (*a*) depicts trajectories of reorientations of the macroscopic optical axis of the cell or the uniformly oriented directors, respectively, during a full cycle of the 200 Hz/1 MV m^{-1} electric square field applied to the cell at several temperatures. The experimental trajectories are evaluated by electro-optical measurements [4, 5]. At 40°C, well below the S_C^*–S_A^* phase transition temperature (44°C); a semicircular trajectory is observed, which indicates a collective and uniform reorientation of the

molecular directors along the director tilt cone at $\Theta \approx$ const. (cf. figure 1) within the optically relevant sections of the cell (tv and bv, cf. figure 2). Deviations from a perfect semicircular shape, representing elliptical and loop-like distortions of the trajectories in figure 3 (*a*), are essentially caused by small variations of the director tilt angle Θ (cf. figure 1) due to the electroclinic effect, which is superimposed on the reorientation along the director tilt cone. With increasing temperature, the director tilt angle Θ of the S_C^* phase decreases and the reorientation along the director tilt cone continuously changes into a small planar motion observed in the S_A^* phase at 45°C, which is caused by a pure electroclinic effect.

This behaviour is reproduced correctly by the proposed model as shown by the theoretically calculated trajectories from the simulations and depicted in figure 3 (*b*). The best fit parameters used for the calculations are listed in the table and will be discussed later.

In order to obtain a direct comparison with experimental results, the calculated director trajectories are converted into the corresponding transmission curves and compared with the electro-optical response of the cell, which was recorded experimentally at an optical wavelength $\lambda_0 = 520$ nm (see figure 4). As concluded from figure 4, the electro-optical response and basic features such as contrast, switching time, threshold behaviour and optical overshoot are well described by the proposed model at all temperatures considered.

Figure 5 depicts the temperature dependence of the Landau potential, determined from the Landau coefficients *a*, *b* and *c* (see the table) by the expansion

$$g - g_0 = \tfrac{1}{2}a\Theta^2 + \tfrac{1}{4}b\Theta^4 + \tfrac{1}{6}c\Theta^6. \tag{3}$$

In the S_A^* phase at 45°C the minimum of the potential is located at $\Theta_0 = 0°$ as expected. At decreasing temperatures the minimum is driven continuously to values $\Theta_0 > 0°$, necessary to represent the formation of the S_C^* phase. The Landau coefficient *a* varies linearly with temperature (see figure 6 (*a*)) as required by theory

$$a = \alpha(T - T_c). \tag{4}$$

Material and cell constants derived from the best fit and used for the simulations at different temperatures.

	T/°C					
	40	41	42	43	44	45
a/kN m^{-2}	−15	−13	−9·5	−5·5	−1·5	40
b/kN m^{-2}	3·9	6·4	9·5	31	356	3500
c/MN m^{-2}	3·9	6·4	9·5	31	356	3500
Φ_0/°				0		
K_{splay}/pN	160	110	50	40	40	40
γ_Φ/Pa s				0·45		
γ_θ/Pa s	1·3	1·9	2·0	2·0	1·7	1·4
γ_{splay}/TPa s m^{-2}				20		
P_0/mC m^{-2}				−1·9		
$\Delta\epsilon_G$	31	26	21	15	12	7
$\Delta\epsilon_S$	0·0	0·5	1·0	4·0	4·0	3

A least squares fit leads to $\alpha = 3800\,\mathrm{kN\,m^{-2}\,K^{-1}}$ and a phase transition temperature $T_c = 44{\cdot}3°\mathrm{C}$. The Landau coefficient b diverges with increasing temperature (see figure 6(*b*)) and is described to a first approximation by:

$$b = \frac{\beta}{|T - T_\beta|^x}. \tag{5}$$

The fit shown in figure 6(*b*) was obtained with $x = 4$, $\beta = 4{\cdot}2 \times 10^6\,\mathrm{N\,K^4\,m^{-2}}$ and $T_\beta = 46°\mathrm{C}$. It is worth noting that at 46°C, first pretransitional changes of the S_A^* texture in the cell are observed. The strong increase of b leads to a limitation of the electroclinic effect, which would otherwise be very large, since the Landau coefficient a vanishes at the phase transition according to equation (4). The Landau coefficient c also diverges for $T \to T_\beta$, as the c/b ratio is found to be constant for all temperatures considered. A more detailed study on the Landau coefficients at the S_C^*–S_A^* phase transition is necessary to clarify the behaviour described. In this context it should be stressed that most of the remaining differences between the experiments and the simulations are due to deviations in the dynamics of the tilt angle during the reorientation. The tilt angle dynamics are essentially controlled by the Landau expansion (see equation (3)) which consequently should be improved for even better results.

The best fit constants used for the simulations are compared with experimental results from various sources and excellent agreement is achieved. X-ray measurements on the temperature dependence of the director tilt angle Θ_0 in the S_C^* phase are depicted in figure 7(*a*), as are the calculated values determined by the minimum of the Landau potentials (see figure 5) with the coefficients a, b, c (see the table).

A comparison between the temperature dependence of the spontaneous polarization calculated from the simulation by

$$P_s = P_0 \sin \Theta_0 \tag{6}$$

and the experimental results from polarization reversal measurements [16] is provided in figure 7(*b*).

The field dependence of the reciprocal switching times leads to an effective rotational viscosity $\gamma_{\Phi,\mathrm{eff}}$ [16] (see figure 7(*c*)), and correlates well with values obtained from the simulation by

$$\gamma_{\Phi,\mathrm{eff}} = \gamma_\Phi \sin^2 \Theta_0. \tag{7}$$

The dielectric strength of the Goldstone mode $\Delta\epsilon_G$ (see the table) is about one order of magnitude smaller than values obtained using thick cells with the helical structure of the S_C^* phase [17, 18]. Obviously, the Goldstone mode fluctuations are mostly suppressed in the surface stabilized arrangement of the cell investigated and the Goldstone mode almost vanishes in the S_A^* phase. In accordance with results from dielectric spectroscopy [17, 18], the dielectric strength of the soft mode $\Delta\epsilon_s$ (see the table) reaches maximal values at the phase transition. The splay elastic constant K_{splay} (see the table) exhibits reasonable values between 10^{-11} and $10^{-10}\,\mathrm{N}$, and a strong increase in the S_C^* phase is observed.

4.2. *Frequency dependence*

Figure 8 depicts the optical response of the cell to a $1\,\mathrm{MV\,m^{-1}}$ electric square field for different frequencies at 41°C and $\lambda_0 = 520\,\mathrm{nm}$. A break down of the electro-optical effect is observed at frequencies above 2 kHz. Below this cut-off frequency, the electro-optical behaviour is well described by the proposed model with one set of constants

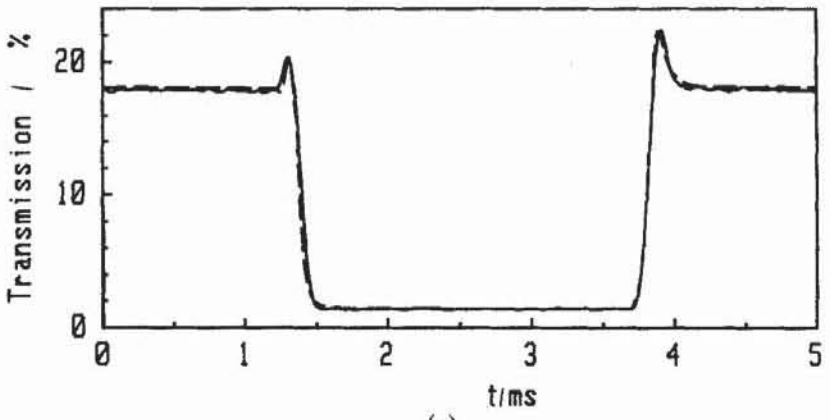
Transmission / %
20
10
0
0
1
2
3
4
5
t/ms

(*a*)

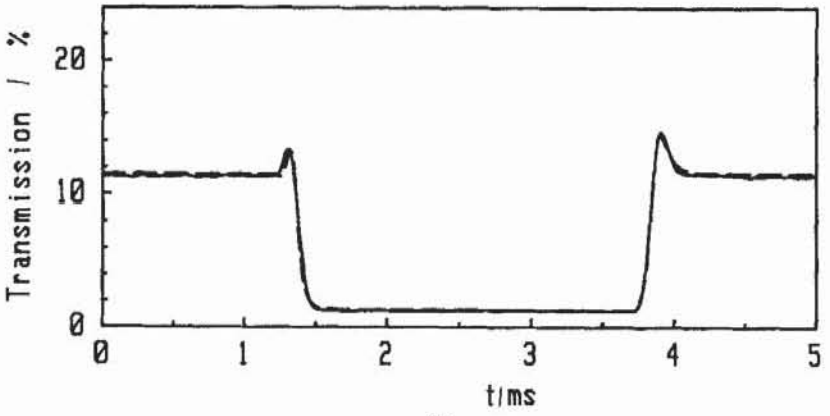
Transmission / %
20
10
0
0
1
2
3
4
5
t/ms

(*b*)

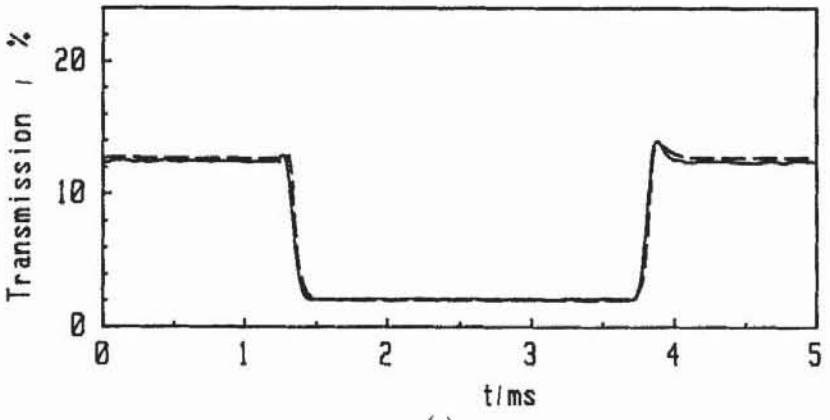
Transmission / %
20
10
0
0
1
2
3
4
5
t/ms

(*c*)

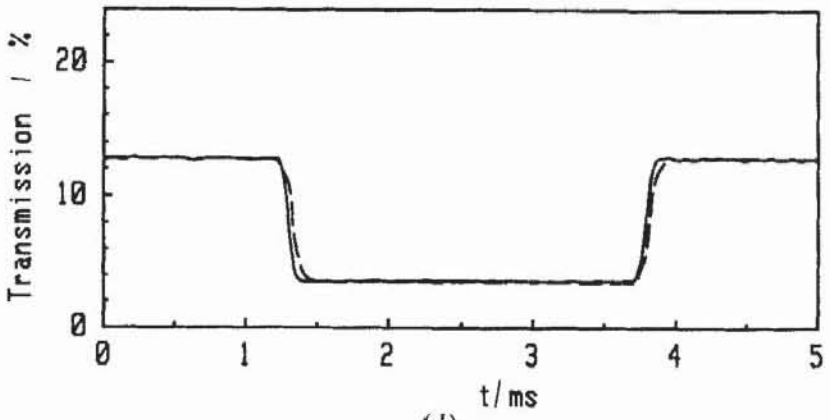
Transmission / %
20
10
0
0
1
2
3
4
5
t/ms

(*d*)

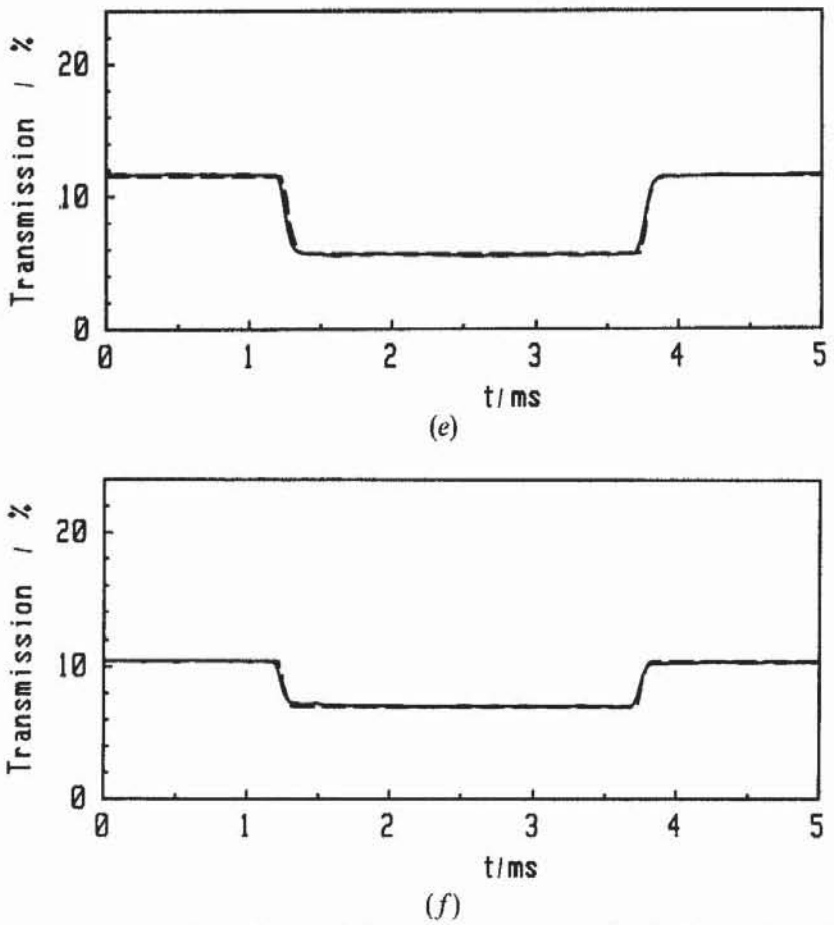

Figure 4. Temperature dependence of the optical response (optical wavelength: 520 nm) to a 200 Hz/1 MV m^{-1} electric square field (solid lines: measurement, dashed lines: simulation; note the almost perfect agreement). (*a*) 40°C, (*b*) 41°C, (*c*) 42°C, (*d*) 43°C, (*e*) 44°C, (*f*) 45°C.

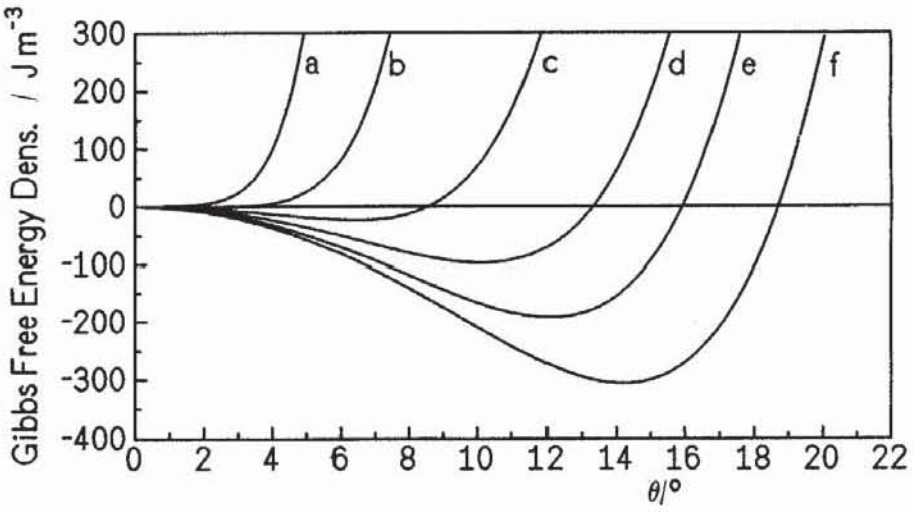

Figure 5. Landau potential obtained from the simulations at different temperatures: $T - T_C =$ +0·7°C (*a*), −0·3°C (*b*), −1·3°C (*c*), −2·3°C, (*d*), −3·3°C (*e*), and −4·3°C (*f*); $T_C = 44{\cdot}3$°C.

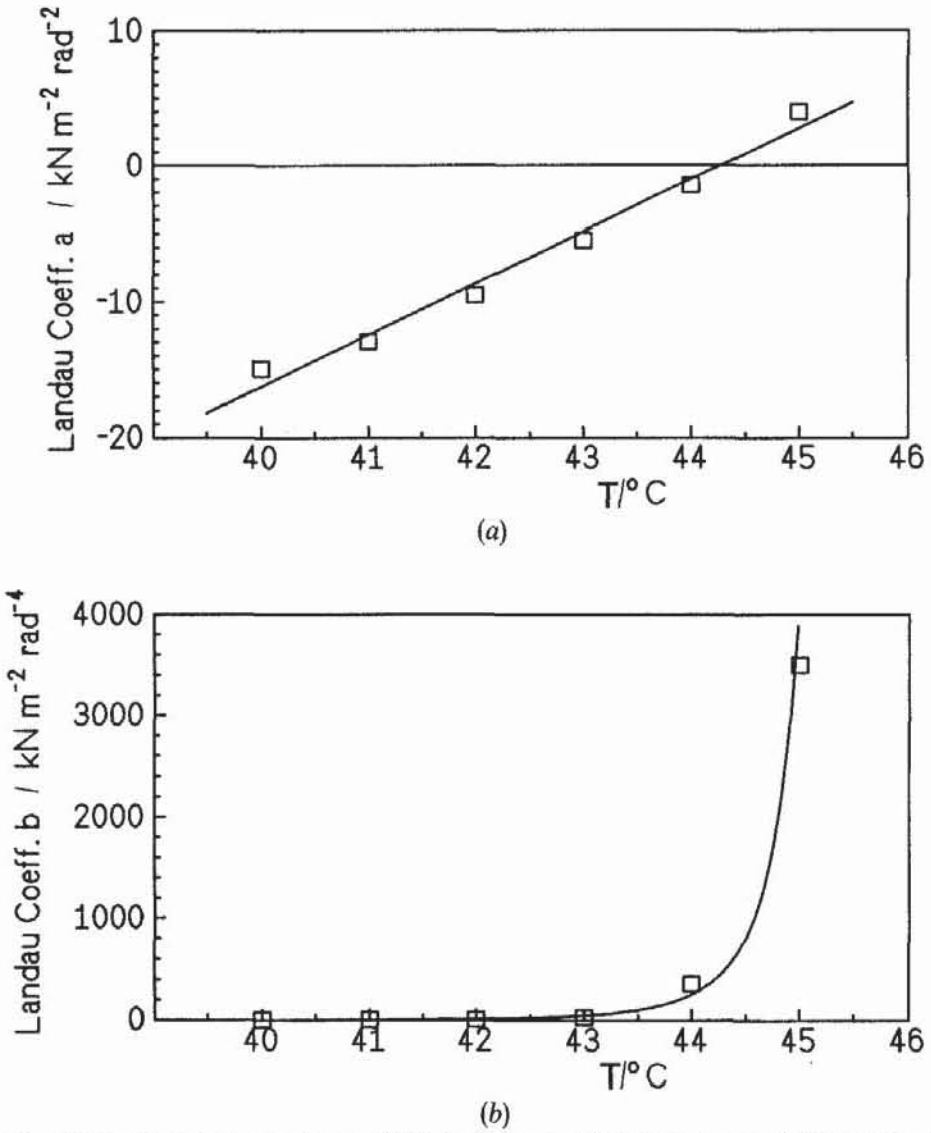

Figure 6. Temperature dependence of the Landau coefficients (*a*) a and (*b*) b obtained from the simulations.

listed in the table for $T = 41°C$. Only the dielectric strength of the Goldstone mode changes between $\Delta\epsilon_G = 26$ at 200 Hz and $\Delta\epsilon_G = 11$ at 2 kHz, due to a relaxation of the Goldstone mode contribution in this frequency range. An estimation of the viscous damping constant γ_{splay}, which applies to the propagation of splay deformations, is discussed in [7].

4.3. *Amplitude dependence*

Figure 9 represents the optical response of the cell to a 500 Hz electric square field at 41°C at various amplitudes. Again, the electro-optical behaviour is well described by the simulations with constants listed in the table for 41°C. At increasing amplitudes of the electric field, a suppression of the Goldstone mode contribution $\Delta\epsilon_G$ from $\Delta\epsilon_G = 25$ at 1 MV m^{-1} to $\Delta\epsilon_G = 6$ at 2·5 MV m^{-1} amplitude is observed. At high amplitudes (see figure 9 (*c*) and (*d*) a slight drift in the transmissions of the stationary switching states is observed, which is not reproduced by the simulations. This drift may be related to deformations at high energy density of the cell, which are not considered in the model used.

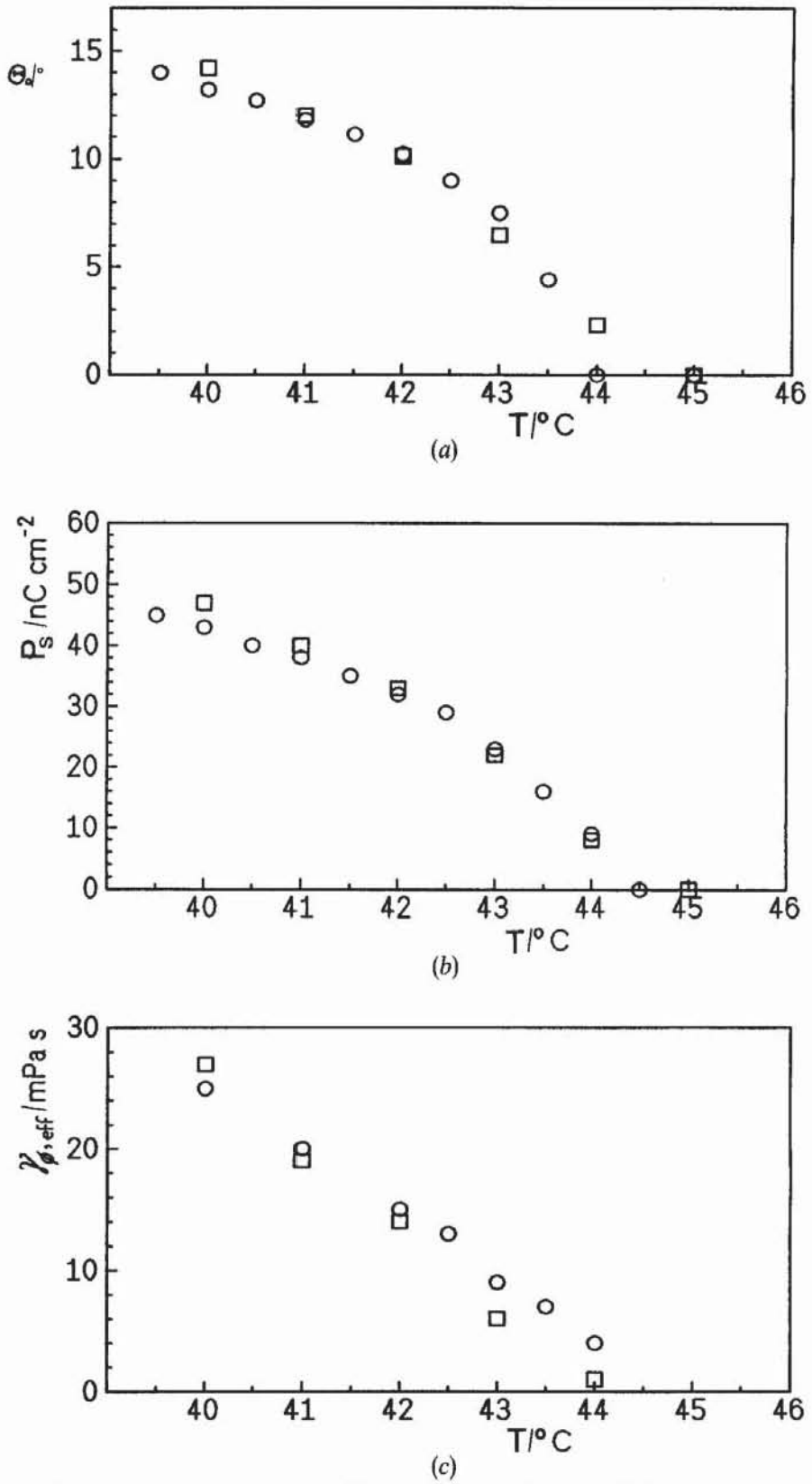

Figure 7. Temperature dependence of (*a*) the director tilt angle (*b*) the spontaneous polarization and (*c*) the effective rotational viscosity; ○, measurement; □, simulation.

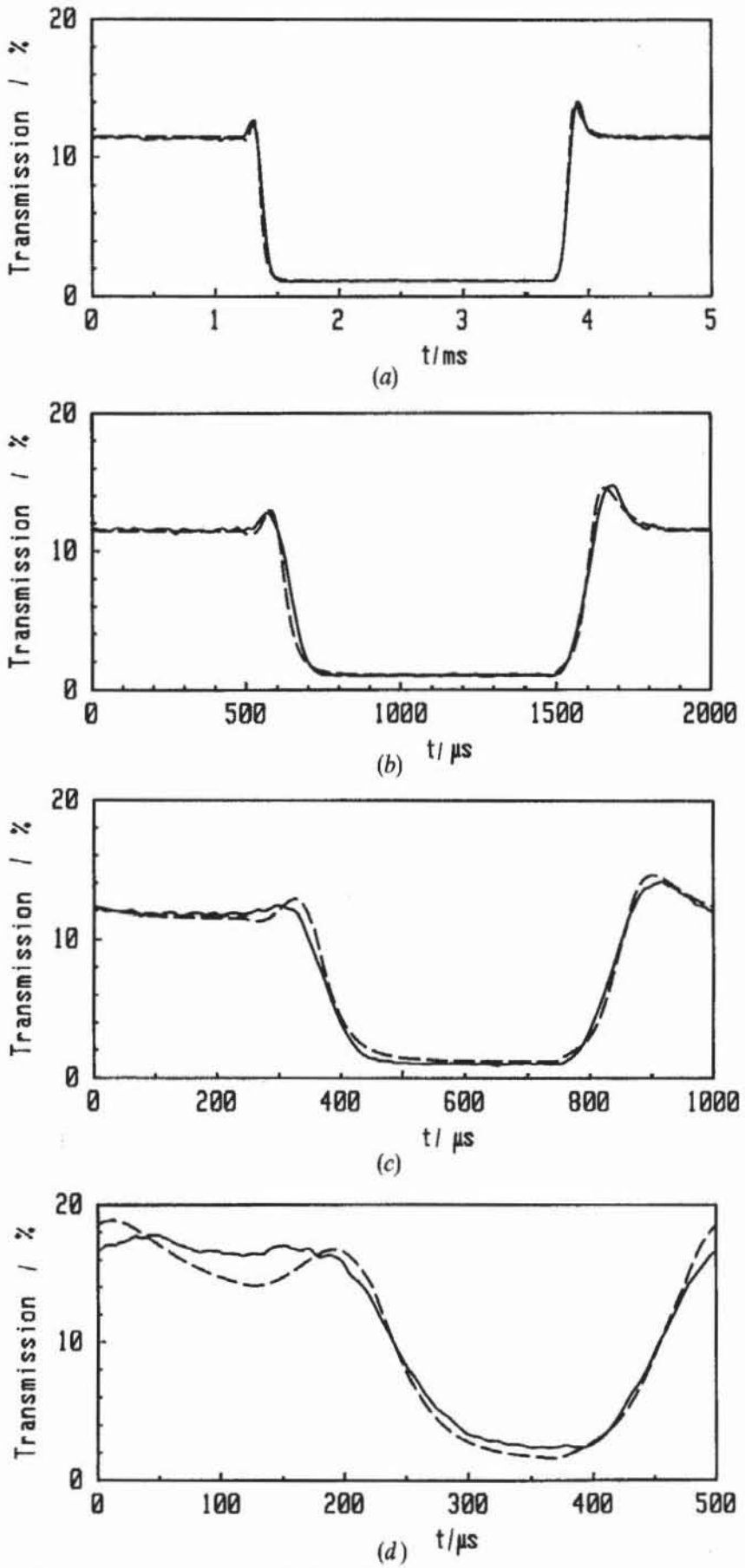

Figure 8. Frequency dependence of the optical response (optical wavelength: 520 nm) to a 1 MV m^{-1} electric square field (solid lines: measurement, dashed lines: simulation) at 41°C; (*a*) 200 Hz, (*b*) 500 Hz, (*c*) 1 kHz, (*d*) 2 kHz.

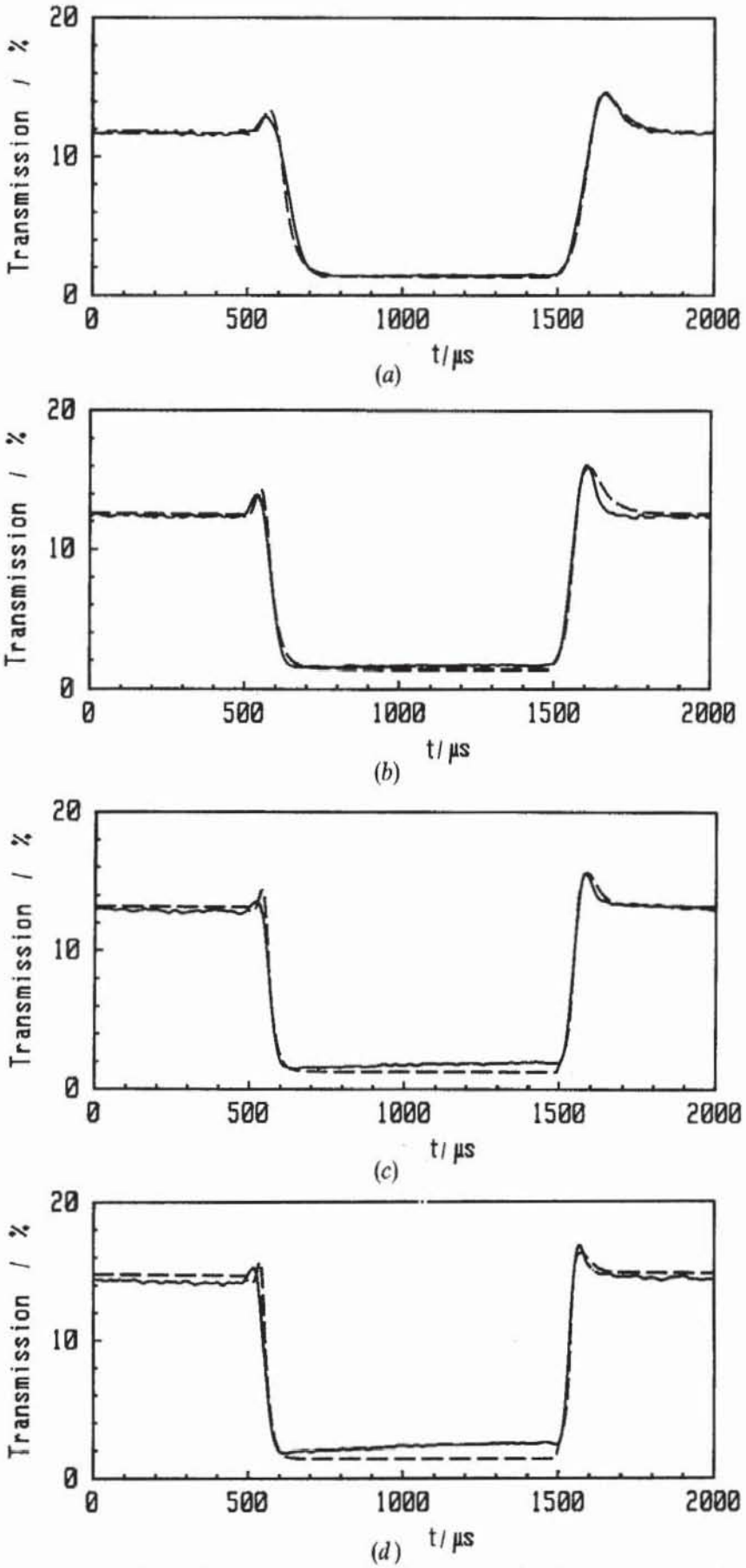

Figure 9. Amplitude dependence of the optical response (optical wavelength: 520 nm) to a 500 Hz electric square field (solid lines: measurement, dashed lines: simulation at 40°C; (*a*) 1 MV m^{-1}, (*b*) 1·5 MV m^{-1}, (*c*) 2 MV m^{-1}, (*d*) 2·5 MV m^{-1}.

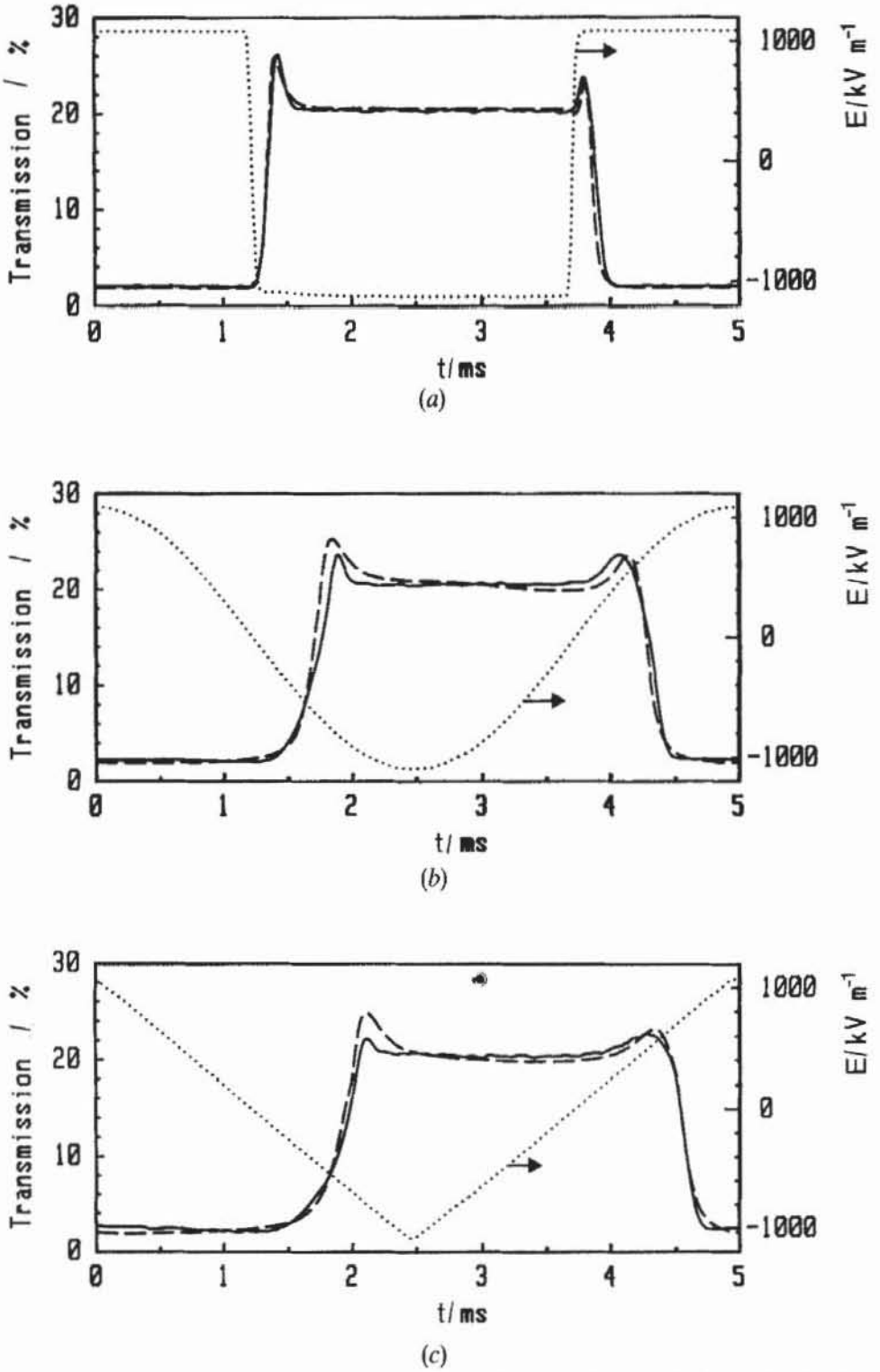

Figure 10. Experimentally determined (solid lines) and simulated (dashed lines) optical response of a 3·6 μm cell to different waveforms of a 200 Hz/1 MV m^{-1} electric field (dotted lines) at 40°C; (*a*) square field, (*b*) sine field, (*c*) triangular field.

4.4. *Dependence on the shape of the applied electric field*

The proposed model also describes the electro-optical response quite well, if changes in waveforms of the electric field applied are considered. Figure 10 depicts the optical response of the cell to three different waveforms of the electric field. The corresponding simulations have been carried out with the constants listed in the table for 40°C. It seems that best agreement between experimental and calculated data sets are obtained for square wave excitation (see figure 10(*a*)), with lesser agreement for sinusoidal (see figure 10(*b*)) and triangular (see figure 10(*c*)) waveforms of the electric field. These deviations are most probably related to a reduced uniformity of the director configuration of the cell at sinusoidal and triangular excitation. The total thickness of the non-uniform layers $\xi_t + \xi_b + \xi_c$ (cf. figure 2) reaches maximal values of 250 nm at square wave excitation, 330 nm at sinusoidal excitation, and 390 nm at triangular excitation. In the latter cases, the uniformity of the cell is reduced and, therefore, leads to some deviations between experiment and simulation.

5. Conclusions

The experimental data and simulation of the reorientational dynamics in surface stabilized ferroelectric liquid crystal cells considered in this investigation provide the following conclusions:

(i) The switching process in these cells may be described optically as uniform director reorientation, if the $\mathbf{P}_s$, $\mathbf{E}$ interaction dominates over the elastic interaction and the propagation of splay deformations is slow compared to the field induced director reorientation. If these conditions are not fulfilled, non-uniform switching models, for example the models discussed in [9, 19, 20], have to be applied. In order to supply a consistent simulation, non-uniform models need much more experimental information (for example the time-resolved spectral response of the cell [9]) than a uniform model, because the whole director configuration has to be considered.

(ii) The proposed model is valid in a frequency range from 10^2 to 10^3 Hz, an amplitude range from 0·5 to 2·5 MV m^{-1} and a temperature range from 40 to 45°C for the system investigated. If the system approaches the S_C^*–S_A^* phase transition, the Landau coefficients b and c diverge.

(iii) The model provides material and cell constants by a best fit to electro-optical data. The validity of this method is supported through the requirement that all measurements, which have been taken at a certain temperature, have to be described with only one set of constants.

(iv) The accuracy of the model might be improved further if the optical influence of non-uniformities are taken into account, and an advanced approach to the tilt angle dynamics is adopted.

This work was supported by a grant from Deutsche Forschungsgemeinschaft.

References

[1] Meyer, R. B., Liebert, L., Strzelecki, L., and Keller, P., 1975, *J. Phys. Lett.*, **36**, L-69.
[2] Meyer, R. B., 1977, *Molec. Crystals liq. Crystals*, **40**, 33.
[3] Clark, N. A., and Lagerwall, S. T., 1980, *Appl. Phys. Lett.*, **36**, 899.
[4] Gießelmann, F., and Zugenmaier, P., 1990, *Liq. Crystals*, **8**, 361.
[5] Gießelmann, F., and Zugenmaier, P., 1990, *Proceedings of the 19. Freiburger Arbeitstagung Flüssigkristalle*, p. 20.

[6] GIEßELMANN, F., and ZUGENMAIER, P., 1991, *Proceedings of the 10. Freiburger Arbeitstagung Flüssigkristalle*, p. 23.
[7] GIEßELMANN, F., and ZUGENMAIER, P., *Molec. Crystals liq. Crystals* (in the press).
[8] GIEßELMANN, F., and ZUGENMAIER, P., 1992, *Proceedings of the 21. Freiburger Arbeitstagung Flüssigkristalle*, p. 44.
[9] MACLENNAN, J. E., CLARK, N. A., HANDSCHY, M. A., and MEADOWS, M. R., 1990, *Liq. Crystals*, **7**, 753.
[10] PATEL, J. S., SIN-DOO LEE, and GOODBY, J. W., 1989, *Phys. Rev.* A, **40**, 2854.
[11] ITOH, K., JOHNO, M., TAKANISHI, Y., OUCHI, Y., TAKEZOE, H., and FUKUDA, A., 1991, *Jap. J. appl. Phys. Lett.*, **30**, 735.
[12] OH-E, M., ISOGAI, M., and KITAMURA, T., 1992, *Liq. Crystals*, **11**, 101.
[13] BRAND, H. R. (private communication).
[14] MOHR, K., KÖHLER, S., WORM, K., PELZL, G., DIELE, S., ZASCHKE, H., DEMUS, D., ANDERSSON, G., DAHL, I., LAGERWALL, S. T., SKARP, K., and STEBLER, B., 1987, *Molec. Crystals liq. Crystals*, **146**, 151.
[15] YANG, K. H., 1988, *J. appl. Phys.*, **64**, 4780.
[16] DIERKING, I., 1992, Diploma Thesis, Institut für Physikalische Chemie, Technische Universität Clausthal.
[17] GOUDA, F., SKARP, K., and LAGERWALL, S. T., 1991, *Ferroelectrics*, **113**, 165.
[18] GOUDA, F., SKARP, K., and LAGERWALL, S. T., 1991, *Molec. Crystals liq. Crystals*, **209**, 99.
[19] MACLENNAN, J. E., HANDSCHY, M. A., and CLARK, N. A., 1990, *Liq. Crystals*, **7**, 787.
[20] ZHUANG, Z., CLARK, N. A., and MACLENNAN, J. E., 1991, *Liq. Crystals*, **10**, 409.